Overview of density flows and turbidity currents

Helmut Knoblauch

June 1999

CONTENTS

1 Introduction

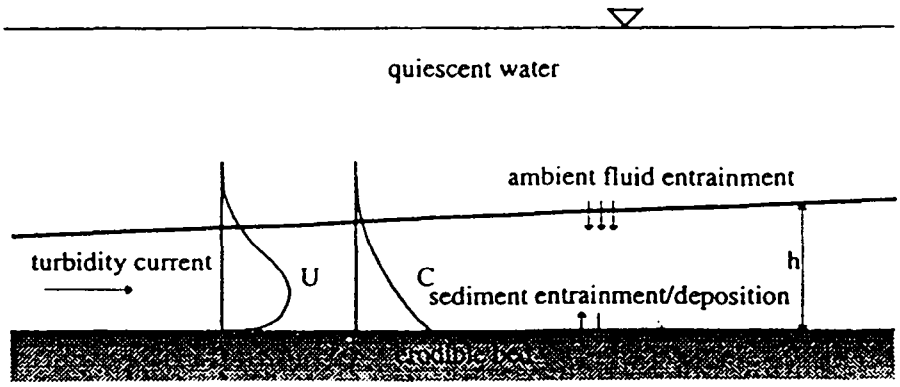

Figure 1: Sketch of typical turbid underflow (Bradford et.al., 1997)

If a fluid of a given density moves into an almost stagnant fluid of slightly different density, it might do this as underflow, interflow or overflow, depending on the density difference. One speaks thus of density currents or gravity currents. Density differences may be caused by temperature, dissolved substances and suspended matters.

Turbidity currents are gravity currents, where the denser phase contains settling granular material. Similar gravity currents can be produced by salinity or temperature differences ("inclined plumes" or "underflows"). In turbidity currents, suspended sediment makes the density of the mixture greater than the density of the ambient water and provides the driving force. The sediment laden flow must generate enough turbulence to hold the sediment in suspension. Density respectively turbidity currents occur in the ocean, in lakes and reservoirs. They may be caused by the direct inflow of turbid water, by wave action, by subaqueous slumps, by the discharge of mining tailings or by dredging operations.

Distinguish between a "conservative gravity current" (the density difference is due to the temperature or the presence of dissolved substances) and a "non-conservative gravity current" (e.g. turbidity current on a mobile bed with deposition or erosion), where the settling velocity of the suspended particles constitute a new parameter, (Altinakar et al. 1990). In general two types of turbidity currents can be distinguished: (I) low velocity, low density, and (II) high velocity, high

density (Akiyama and Stefan 1984). They are characterized by a distinctive raised head, followed by a quasi-uniform flow region ("body"). The dynamics of a turbidity current can have a major impact on the water quality and sedimentation of lakes and reservoirs (Bruk 1985).

2 Characteristics

2.1 General

Turbidity currents can be erosive or depositional. The flow itself is taken to be essentially two-dimensional. Some examples for turbidity currents besides hydraulics are dust storms in deserts, pyroclastic flows of volcanos, powder-snow avalanches and large scale marine turbidity currents resulting from land slides.

Ordinarily the velocity of a turbidity current is less than 1.0 ft/s (0.30 m/s). But much higher velocities have been reported by (Brown, 1943) – from 0.10 ft/s to 3.0 ft/s, occurred on slopes as low as 0.002%. Thereby the sediment concentrations ranged from 7.8% to as low as 0.007% and the depth of the currents from a few inches up to more than 100 ft. (30 m).

Turbidity currents differ from the simple conservative underflows (Ellison and Turner 1959) in that the source of the buoyancy difference (i.e. the suspended sediment) is not conserved. Suspended sediment is free to exchange with bed sediment. This exchange must be quantified in terms of bed erosion and deposition. Turbulent energy is expended in both maintaining the existing load in suspension, and entraining new sediment from the bed.

Density currents will reach a normal state within a short distance. In a normal state, gravity force, bottom shear, pressure force and momentum due to water entrainment are in balance. The Richardson number assumes a normal value after a short distance. In turbidity currents there are additional terms in the governing equations (erosion, deposition). The Richardson number requires a much longer distance to become at least normal.

Richardson's number $$Ri = \frac{g' h_b}{u_b^2}$$

There are 3 basic types of turbidity currents: (I) accelerating erosive (II) decelerating erosive (III) decelerating depositive. In accelerating erosive turbidity currents the velocity and Richardson number approach the same values as in density currents:

On a constant slope, density currents never cease, but turbidity currents do, because (I) the flow becomes subcritical (Ri > 1), which must lead to deceleration and sediment deposition and/or (II) deposition occurs even in supercritical flow (Ri < 1) if the size of the sediment particles is large enough. Gravity currents without sediment are flows whose initial buoyancy flux is preserved. The buoyancy flux of a turbidity current is not conserved (disequilibrium in sediment concentration makes turbidity currents eroding or depositing, accelerating or decelerating) (Akiyama and Stefan 1988)

Density currents are caused by density differences due to temperature, total dissolved solids and suspended solids. For example, at 25°C (77 F) it takes approximately 330 mg/l of dissolved solids or 420 mg/l of suspended solids ($\rho = 2.65$) to equal the density difference caused by 1°C temperature change (Ford and Johnson 1983).

2.2 Influencing variables

2.2.1 Complicated morphometry

I.e. coves, embayments, islands. Several field observations showed that density currents were not well-mixed laterally but followed the thalweg of the innundated river

2.2.2 Unsteady and multiple inflows

Dependent on the size and shape of the watershed, antecedent conditions, distribution of precipitation. The density of the inflowing water (as a function of temperature, suspended solids and total dissolved solids) is also variable. Water temperature varies seasonally, synoptically (i.e. for periods of 5-10 days) and diurnally. Also take care of the unique thermal-density properties of water (maximum density at 4°C).

2.2.3 Variable stratification

The in-lake stratification varies in response to hydrometeorologic forcing, but not at the same rate as the tributary. The larger volume of water in the lake responds at a slower rate than the river water. Typically overflows occur in the spring (the river water warms at a faster rate) and interflows and underflows occur in late summer and fall (river water cools at a faster rate). There can be changes in stratification occuring during storm events and a nocturnal and seasonal convective mixing.

2.2.4 Hydraulic jump in a turbidity current

The amount of water entrained by the flows through a hydraulic jump is small. In nature, a turbidity current experiencing a hydraulic jump will drop most of its bedload immediately downstream from the jump, while the suspended load will respond more gradually to the change in flow regime and will deposit sediment over a distance far exceeding 1000 times the jump height. A marked reduction of the bed shear stress occurs downstream of the hydraulic jump(Garcia 1993).

2.2.5 Other variables

Inflows can carry solids, nutrients, bacteria and other substances that affect reservoir water quality. When inflow enters a wide lake (i.e., width > 1 km) in the northern hemisphere, Coriolis accelerations cause the density interfaces to tilt to the right side of the basin.
(Thornton et al. 1981) have proposed a heuristic model which divides a reservoir into (see fig. 2)

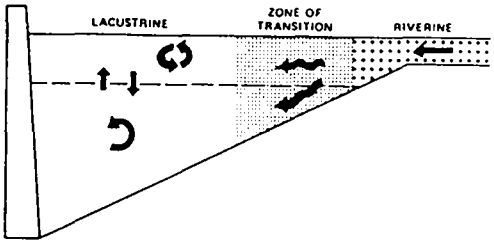

Figure 2: Division of a reservoir after (Thornton et al. 1981)

I. Riverine zone : Current velocities are decreasing but the advective forces are still sufficient to maintain a well-mixed environment.

II. Transition Zone: The buoyancy forces begin to dominate over the advective forces and the inflow plunges. The upstream and downstream boundaries of the transition zone may correspond with the location of the plunge point under low-flow and high-flow conditions, respectively.

III. Lacustrine Zone: Buoyancy forces dominate and inflow move through the reservoir in well defined horizontal layers as interflows and underflows.

3 Plunge Point

3.1 General

Density currents respectively turbidity currents enter a reservoir, plunge beneath the clear water, and travel downstream along the submerged thalweg. The zone where the inflowing turbid water entering a reservoir plunges beneath the ambient water, thereby producing stratified flow, is called the plunge point or plunge line. In a narrow reservoir the plunging flow will form a line across the width of the reservoir. When a sediment-laden flow discharges into a wide reach, the turbid surface water may extend into the reservoir as an irregular tongue-like current which can shift from one side of the impoundment to the other.

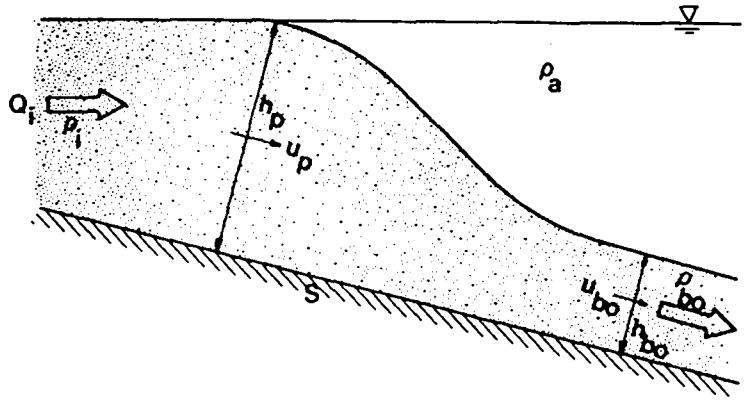

Figure 3: Definitions at the plunge point (Ford and Johnson 1983)

3.2 Plunge point location - general

The location of the plunge point is determined by a balance between the stream momentum, the pressure gradient across the interface separating the river and reservoirs water, and the resisting shear forces. The location of the plunge point can also be influenced by morphological factors (bed slope, bed friction, cross-sectional area). The location is highly dynamic. It can move several kilometers in a few hours in response to dynamic flow events (storm event, hydropower generation).

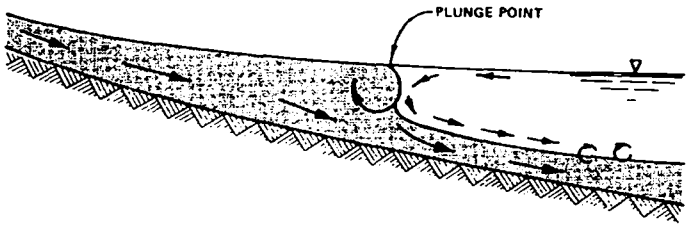

Figure 4: Large eddies formed by flow reversals in the vicinity of the plunge point (Ford and Johnson 1983)

Some mixing (termed initial mixing) occurs at the plunge point because of the large eddies formed by flow reversals and pooling of the inflowing water (Akiyama and Stefan 1981). The flow in the vicinity of the plunge point occures at the bottom of this pool mixing (see figure 4).

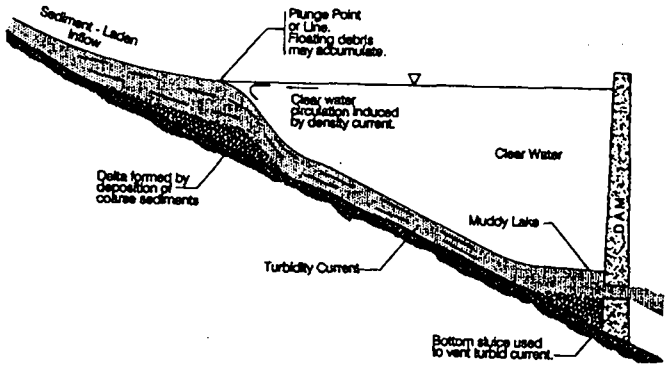

Figure 5: Schematic diagramm of the passage of a turbid density current through a reservoir (Morris and Fan 1998)

After the inflow plunges, it follows the old river channel (thalweg) as an underflow (figure 5). The speed and thickness of the underflow is determined by a flow balance between shear forces and the acceleration due to gravity (i.e. gradually varying flow theory).

3.3 Plunge point location after Morris and Fan

The water depth at the plunge point can be estimated based on the densimetric Froude number at the plunge point F_P:

$$F_P = \frac{v}{\sqrt{\frac{\Delta\rho_i}{\rho_a} g h_P}}$$

The above equation for the densimetric Froude number can be rearranged to determine the depth h_P at the plunge point by assuming a rectangular cross section with a bottom width B:

$$h_P = \left(\frac{Q}{F_P B}\right)^{2/3} \left(\frac{\Delta\rho}{\rho_a} g\right)^{-1/3}$$

Both flume tests and measurements in reservoirs indicate that F_P has a value of about 0.78 at the plunge point. Values of densimetric Froude numbers reported by various researchers are summarized in table 1 (Morris and Fan 1998).

Author	Laboratory or field data	F_P
Bu et al., 1980	Liujiaxia Reservoir, Tao River	0.78
Fan, 1991	Guanting Reservoir	0.5 – 0.78
Fan, 1960	Turbid water flume tests:	
	3-19g/l	0.78
Cao et al, 1984	Turbid water flume tests:	
	10-30 g/l	0.55 – 0.75
	100-360 g/l	0.4 – 0.2
Singh and Shan, 1971	Saline water	0.3 – 0.8
Farrel and Stephan, 1986	Cold water	0.67

Table 1: Densimetric Froude Number F_P at Plunge Point (Fan and Morris 1998)

3.4 Plunge point location after Singh and Shah

(Singh and Shah 1971) conducted an experimental study of the plunging phenomenon on using a tilting flume with salt water flowing into a reservoir filled with tap water. Using the method of least squares, they related the plunge point depth, h_P, to the critical depth by the equation:

$$h_P = 0.0185 + 1.3\left(\frac{q_i^2}{g\varepsilon_i}\right)^{1/3}$$

They also investigated the plunging phenomenon analytically. Applying the momentum principle across the transition region (see fig. 3) they were able to derive an equation similar to the equation for conjugate depths of a submerged hydraulic jump. Substituting experimental values for friction, they reduced the momentum equation to:

$$(h_P + h_{b0})(h_P\, h_{b0}) = 3.1\frac{Q_i^2}{g}$$

Assuming h_P is similar to h_{b0}, then this equation reduces to:

$$h_P = 1.16\left(\frac{q_i^2}{g\varepsilon_i}\right)^{1/3}$$

3.5 Plunge point location after Savage and Brimberg

(Savage and Brimberg 1975) analyzed plunging phenomena in two ways: the first was based on conservation of energy and the second on gradually varied flow theory in a two-layered stratified system.

In the simple energy balance, interfacial and bed friction as well as slope were neglected. The flow in the upper layer was assumed to be zero. The Froude number at the plunge point was found to be 0.5, which resulted in a plunge point depth of:

$$h_P = \left(\frac{q_i^2}{g\varepsilon_i}\right)^{1/3}$$

In the two-layered analyses, the authors used the one-dimensional equations of motions for gradually varying flow (Schuijf and Schoenfeld 1953). These equations included bed slope and interfacial and bed friction and were used to define the shape of the interface. For the case where flow in the lower layer reaches normal depth downstream of the plunge point, the equation was integrated numerically to determine the Froude number as a function of slope and roughness. That is,

$$F_P \cong \frac{2.05}{(1+\alpha)}\left(\frac{S}{f_b}\right)^{0.478}$$

3.6 Plunge point location after Hebbert et al.

The authors considered a triangular cross section with half angle ϕ (see figure 6). Starting with the equations for conservation of volume and momentum, they related the downstream normal densimetric Froude number, F_{b0}, to the ratio between h_{b0} and the plunge point depth h_P. There is a unique relationship between width and longitudinal distance and the predicted plunge depth corresponding to the maximum reservoir depth.

$$h_{b0} = \left(\frac{2Q_i^2}{F_{b0}^2\, g\, \varepsilon_i \tan^2\phi}\right)^{1/5}$$

With the use of the parameter ς [$\varsigma = h_{b0}/h_P$ $(0.96 < \varsigma < 0.98)$] one can determine the depth at the plunge point h_P.

The normal depth densimetric Froude number downstream of the plunge point, F_{b0}, is given by:

$$F_{b0}^2 = \frac{\sin S \tan\phi}{C_D}\left(1 - 0.85 C_D^{0.5} \sin S\right)$$

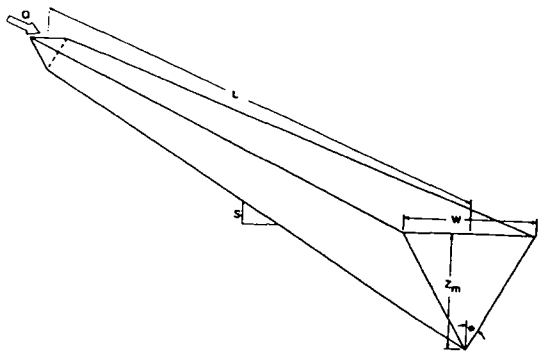

Figure 6: Consideration of a triangular cross section (Hebbert et al. 1979)

3.7 Plunge Point location after Jain

Jain examined the gradually varied two-layer flow analysis of (Savage and Brimberg 1975) and assuming the mean velocity in the upper layer is zero. He concluded that the interfacial profile calculation was sensitive to the direction of numerical integration. The equations should be integrated in the direction in which the hydraulic control is acting. For mild slopes, which are characteristic of most reservoir systems, the hydraulic control is downstream and the integration should start downstream, not at the plunge point.

Based on the gradually varied two-layer flow analysis, Jain proposed a nondimensional formula for the plunge point depth

$$\frac{h_P}{h_n} = 1.6\left(\frac{\alpha}{1+\alpha}\right)^{0.126}\left(\frac{h_c}{h_n}\right)^{0.024}$$

By rearranging the above mentioned equation, you will get for the plunge depth:

$$h_P = 0.814\left(\frac{\alpha}{1+\alpha}\right)^{0.126}\left(\frac{f_i + f_b}{S}\right)^{0.325}\left(\frac{q_i^2}{g\varepsilon_i}\right)^{1/3}$$

3.8 Plunge Point location after Akiyama and Stefan

(Akiyama and Stefan 1981) proposed a conceptual flow model for the plunge point which depends on inflow conditions (densimetric Froude number), downstream conditions (Channel slope, roughness and width) and mixing. Starting with the integrated momentum equation and assuming steady flow, they determined the plunge depth (for a mild slope):

$$h_P = 1.1(1+\gamma)\left(\frac{f_i}{S}\right)^{1/3}\left(\frac{q_i^2}{g\varepsilon_i}\right)^{1/3}$$

3.9 Plunge point location after Ford and Johnson (General form)

All of the models locate the plunge point by calculating the hydraulic depth at which the inflow plunges, which can be put in the general form:

$$h_P = \left(\frac{1}{F_p^2}\right)^{1/3}\left(\frac{Q_i^2}{W_c^2\, g\varepsilon_i}\right)^{1/3}$$

Once F_P is determined, the plunge depth can be calculated from the above equation in an iterative fashion by assuming a width (which is not constant in a reservoir) and calculating the depth.

4 Stability of density currents

The stability of interfacial waves is mainly governed by two parameters, the characteristic Reynolds and Froude numbers, since the phenomenon is governed by viscosity and gravity . (Garde and Ranga Raju 1977)

For turbidity currents of the underflow type, these parameters take the form

$$R_e = \frac{v\, h_{b0}}{\nu} \qquad \text{and} \qquad F_{b0} = \frac{v}{\sqrt{\frac{\Delta\rho_i}{\rho_a} g\, h_{b0}}}$$

(Keulegan 1949) and (Rouse 1950) have shown that the parameter θ governs the stability of interfacial flows:

$$\Theta = \frac{\nu g(\Delta\rho/\rho_f)}{v^3} = \frac{1}{F_i^2}\frac{1}{R_e}$$

According to (Rouse 1950) underflows are stable if

$$R_e \cdot F_{r1}^{3/2} < 440$$

(Ippen and Harleman 1952) have conducted experiments concerning underflows. Their data when plotted with $\theta^{1/3}$ as ordinate and R_e as abscissa show that, for laminar flows to be stable:

$$\theta > 1/R_e$$

(Keulegan, 1949) has given the critical value (see figure below)

- for laminar flows: $\theta < 0.127$
- for turbulent flows: $\theta < 0.178$

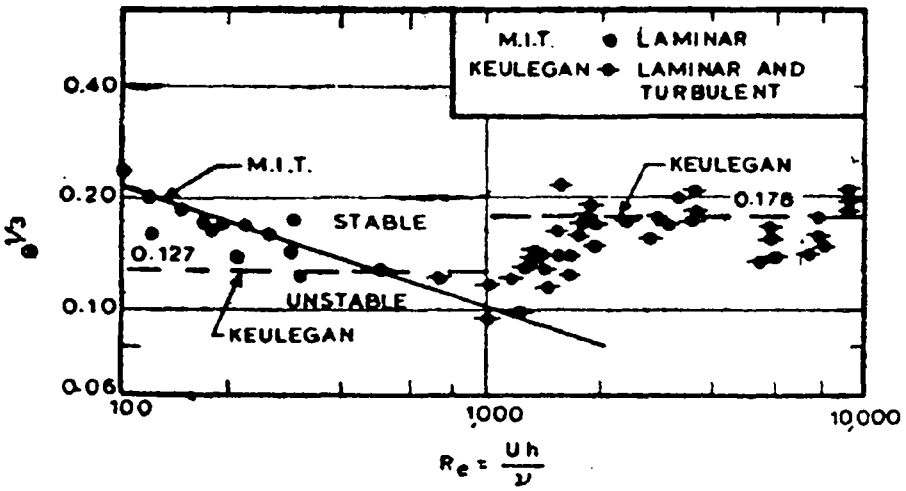

Figure 7: Stability criteria for underflows (Garde and Ranga Raju 1977)

5 Initial mixing and ambient fluid entrainment

5.1 Initial mixing

Initial mixing includes the cumulative effects of all mixing processes acting in the vicinity of the plunge point. Entrainment occurs at the interface between the underflow and reservoir water after the inflow has plunged. Turbulence generated by bottom roughness entrains reservoir water into the underflow.

Water tends to pool at the plunge point, since it flows into the plunge zone faster than it flows out

creating a large eddy (Ford and Johnson 1983). Q_{b0} is described as the revised flow rate including entrainment downstream of the plunge point, whereby ρ_{b0} is the revised inflow density after entrainment at the plunge point.

$$Q_{b0} = (1+\gamma)Q_i$$

The entrance mixing coefficient γ is expected to be a function of the densimetric Froude number for F_n>0.167 (Jirka and Watanabe 1980):

$$\gamma = 1.2\, F_n - 0.2$$

For reservoirs characterized by mild slopes (10^{-3}), initial mixing and entrainment are small, averaging about 25%.

5.2 Ambient fluid entrainment

Entrainment rates for an underflow can be calculated from field data using conservation of volume (Ford and Johnson 1983):

$$\frac{\partial A}{\partial t} + \frac{\partial}{\partial x}(u_{b0}\, A) = E\, u_{b0}\, B$$

$$E = 0.0015\, Ri^{-1} \quad \text{(Ashida \& Egashira, 1977)}$$

$$E = \frac{\eta^3\, C_K\, C_b^{1.5}\, F_{b0}^2}{2} \quad \text{(Imberger \& Patterson, 1981)}$$

$$\text{where } Ri = \frac{\Delta\rho_i}{\rho_a}\frac{g\, h_{b0}}{u_{b0}^2} = \frac{1}{F_{b0}^2}$$

6 Overflows, intrusions and underflows

6.1 Overflows

Overflows occur when the inflowing water density is smaller than the reservoir water surface density. (Safaie 1979) found in a series of laboratory experiments the following empirical equation for the separation depth h_P:

$$h_P = 0.914\, h_i\, (F_i)^{1/2}$$

$$F_i = \frac{u_i}{\left(\frac{\Delta\rho_i\, g\, h_i}{\rho_a}\right)^{1/2}}$$

The above equation is valid for $F_i > 1.2$. If $F_i < 1.2$, then $h_P < h_i$, indicating the plunge point moves up. Here the plunge point can be assumed to occur at the upper end of the reservoir. For $F_i > 3$, the horizontal spreading can be assumed by the following equation (Safaie 1979).

$$W_x = W_0 + K\,x$$

Assuming shear is small and the flow regime is governed by a balance of inertial and buoyant forces, the following equation describes the propagation speed of the overflow (Koh 1976).

$$u_s = \frac{L_s}{t} = \left(\frac{\frac{6}{\pi}\frac{\Delta\rho_i}{\rho_a} g\, q_i}{1 + \frac{3}{2} C_P}\right)^{1/3}$$

The overflow thickness h_s can be obtained from:

$$h_s = 1.24\left(\frac{q_i^2}{g\frac{\Delta\rho_i}{\rho_a}}\right)^{1/3}$$

6.2 Underflows

The depth respectively thickness of the underflow is determined by the discharge, the density of the flow, and the bed and interfacial friction. For the bottom slope $S < 0.67\%$ (for a total friction factor $f_t = 0.02$) the underflow will remain subcritical.

The integral method for analyzing the 2-d underflow is used to assume the shape of the velocity and density profiles. Then, for an elemental volume of unit width, consider:

- the conservation of momentum
- the conservation of volume

- the conservation of mass.

For uniform flow which is achieved downstream for mild slopes the depth/thickness of the underflow will be (Ellison and Turner 1959)

$$h_b = \frac{\beta}{R_n}(x - x_0) + h_{b0} = E(x - x_0) + h_{b0}$$

$$R_n = \frac{\frac{1}{2}S_1\beta + f_t + \left[\left(\frac{1}{2}S_1\beta + f_t\right)^2 + 4\beta S_2 \tan\phi\right]^{1/2}}{2S_2 \tan\phi}$$

6.3 Interflows and intrusions

A density interflow or intrusion occurs when a density current leaves the river bottom and propagates horizontally into a quiescent startified fluid. The density current enters the stratified fluid at the level where the densities of the two fluids are equal. Once the intrusion enters the stratified water column, all turbulence (e.g. bottom generated) quickly collapses and the intrusion assumes the properties of the water column. The density of the underflow at the depth where the density current enters the water column and becomes an intrusion may not be the same as the density of the river water entering the reservoir, because of the initial mixing and entrainment. Changes in flow rate and density of the current due to initial mixing and entrainment must therefore be known before an intrusion can be analyzed (Ford and Johnson 1983).

7 Analytical approach

7.1 Governing equations

A steady, continuous turbidity current is flowing downslope through a quiescent body of water which is assumed to be infinetly deep and unstratified except for the turbidity current itself (see figure 8). The cross section is taken to be rectangular, with a width many time larger than the underflow thickness, so that variations in the lateral direction can be neglected. The bed has a constant, small slope S and is covered with sediment.

The equations of fluid mass, sediment mass and momentum balance provide a theoretical

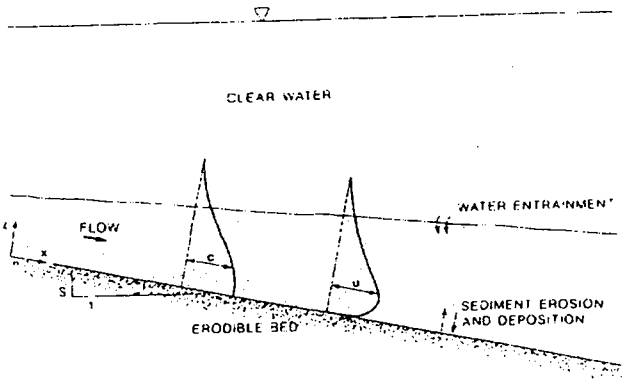

Figure 8: Turbidity current flowing downslope a reservoir (Garcia 1994)

model for steady, continuous turbidity currents laden with poorly sorted sediment (Garcia 1994). These equations form a coupled system of nonlinear, hyperbolic, partial differential equations (mathematically similar to the compressible Euler equations as well as the shallow-water equations) The correct speed of the propagating wave could be obtained by either including a turbulent entrainment term in the continuity equation, or by specifying a finite acceleration of the wave front.

Following these equations, the parameters for the layer-averaged equations of motion for non-conservative turbid underflows are (Parker et al. 1986) flow velocity, volumetric concentration of suspended sediment, layer thickness and the level of turbulence (mean turbulent kinetic energy per unit mass).

The auxiliary parameters are the velocity of entrainment of clear water (use of Richardson number), the near-bed volumetric sediment concentration (averaged over turbulence, related to the layer-averaged concentration by a shape factor), the bed shear velocity and the vertical volumetric Reynolds flux of suspendet sediment (sediment entrainment coefficient - a function of bed shear stress and sediment characteristics).

7.2 Equations of fluid mass, sediment mass and momentum balance

Equation of fluid mass:

$$\frac{d\,U\,h}{d\,x} = e_w\,U$$

Equation of sediment mass balance in layer-averaged form (by summing over all sizes):

$$\frac{d\,U\,C\,h}{d\,x} = \sum_{i=1}^{n} v_{Si}\left(E_{Si}^{*} - c_{bi}\right)$$

Equation of momentum balance by adopting the "top hat" (Turner 1973) or "slab" (Pantin 1979) assumption (U, V, C_i are constant over the thickness h):

$$\frac{d\,U^2\,h}{d\,x} = g\,\Delta\rho\,C\,h\,S - \frac{1}{2}g\,\Delta\rho\frac{d}{d\,x}\left(C\,h^2\right) - u_*^2$$

7.3 Description of the auxiliary parameters

The above proposed theoretical model must be closed with algebraic laws for the water entrainment coefficient, the bed shear stress, the near-bed volumetric sediment concentration and the sediment entrainment coefficient.

The water entrainment coefficient e_w is known to be a function of the bulk Richardson number Ri, which is equal to the reciprocal of the square of the densimetric Froude number

For instance, the following expression was proposed by (Parker et al. 1987):

$$e_w = \frac{0.075}{\left(1 + 718\,Ri^{2.4}\right)^{0.5}}$$

The bed shear stress u_* can be taken to be proportional to the square of the velocity (Turner 1973):

$$u_*^2 = f_b\,U^2$$

The near-bed sediment concentration c_{bi} can be related to the layer-averaged concentration C_i by a shape factor r_{0i}. A good similarity collapse is observed when the concentration profiles for the different grain sizes are normalized in terms of the near-bed concentration c_{bi} measured at z = 0.05h (Garcia 1990).

$$c_{bi} = r_{0i} C_i$$

The shape factor r_{0i} of the near-bed sediment concentration c_{bi} can be obtained by

$$r_{0i} = r_0 g_0(\delta_i)$$

Since for uniform sediment $r_0 \approx 2$, a relationship for $g_0(\delta_i)$ can be obtained as follows:

$$g_0 = 0.20\,\delta_i^{1.64} + 0.82$$

The sediment entrainment coefficient E_{si}^* can be evaluated as

$$E_{si}^* = p_i E_{si}$$

7.4 "Backwater" relations for turbidity currents

With the help of the auxiliary parameters the equations of fluid mass, sediment mass and momentum balance can be cast in the following form:

$$\frac{dh}{dx} = \frac{-RiS + C_D + e_w\left(2 - \frac{Ri}{2}\right) + \frac{Ri}{2}\sum r_{0i}\frac{v_{si}}{U}\frac{\psi_i}{\psi}\left(\frac{\psi_{ei}}{\psi_i} - 1\right)}{(1 - Ri)}$$

$$\frac{h}{U}\frac{dU}{dx} = e_w - \frac{dh}{dx}$$

$$\frac{h}{\psi}\frac{d\psi}{dx} = \sum r_{0i}\frac{v_{si}}{U}\frac{\psi_i}{\psi}\left(\frac{\psi_{ei}}{\psi_i} - 1\right)$$

8 Field studies and laboratory tests

8.1 Field Studies

Only a few direct observations of turbidity currents in the field have been made (Weirich 1986), (Chikita 1989). About the problems of field measurements see (Inman et al. 1976), (Lambert and Giovanoli 1988).

8.2 Laboratory Tests

Laboratory tests on turbidity currents have been made by (Kuenen and Migliorini 1950); (Michon et al. 1955); (Middleton 1967); (Tesaker 1969); (Stefan 1973); (Ashida and Egashira 1975); (Luthi 1981); (Palesen 1983); (Siegentaler and Buhler 1985); (Parker et al. 1987); (Middleton and Neal 1989); (Altinaker et al. 1990); (Garcia and Parker 1993). Most studies have concentrated on turbidity current laden with uniform-size material. For studies on turbidity currents laden with poorly sorted sediment see (Garcia 1994).

On horizontal slopes, for turbid and saline gravity currents the head velocity is slightly decelerating (Altinakar et al. 1990). On finite slopes (S<3.6%) the head travels with about constant velocities. In detail: for turbidity currents the velocity of the head shows a slight deceleration, possibly related to the ratio of sediment fall velocity to velocity of the head. For saline gravity currents you can observe a slight acceleration of the head (Altinakar et al. 1990).

Calculation of the head can be done by a Chezy-type relationship (Altinakar et al. 1990):

$$U_f = C_C \sqrt{g_f' H_f}$$

The calculation of the head can also be expressed as a function of the initial buoyancy flux, the slope angle and the Reynolds number (Altinakar et al. 1990).

(Britter and Linden 1980) consider that there is a finite, critical value of the slope angle, below which the buoyancy can no longer balance the bottom drag, therefore the head is decelerating.

9 Notation

A = cross sectional area of the flow
B = top width of the underflow
C = sum of layer-averaged concentrations corresponding to each sediment size range, i.e.: ΣC_i
C_b = bottom drag coefficient; C_b = 0.015 (Imberger and Patterson 1981)
c_{bi} = near bed concentration of material in the i-th size range
C_C = coefficient for determining the velocity of the head of an underflow
C_C = 0.75 and 0.63 for small slope range
$C_D = (f_b + f_i)/4$ = drag coefficient; values of C_D for turbidity currents have been found to vary between 0.002 and 0.05 (Parker et al. 1987); the lower values correspond to observations in reservoirs, and the higher values to laboratory experiments.

C_i = layer-averaged volumetric concentration of sediment in i-th size range
C_P = coefficient to account for nonhydrostatic pressure distribution ($C_P = 0.5$ from laboratory tests for a surface source)
D_i = diameter of sediment in *i*th size range
D_{sg} = geometric mean size
E = entrainment coefficient (function of the Richardson number)
E_{si} = entrainment coefficient for a bed fully covered by sediment in the i-th size range, which is known to be a function of the bed shear stress and sediment characteristics; relationships to estimate E_{si} can be found in (Garcia and Parker 1991)
E_{si}^* = dimensionless coefficient for the entrainment into suspension of bed material in the i-th size range (Garcia and Parker 1991)
e_W = water entrainment coefficient
f_b = bed friction coefficient;
f_i = interfacial friction coefficient
F_i = inflow Froude number
F_P = densimetric Froude number at the plunge point, $(0.1 < F_P < 0.7)$
$f_t = f_b + f_i$ = total friction factor
$g' = g(\rho_i - \rho_a)/\rho_a$ = relative acceleration of gravity
$g_0(\delta_i)$ = a function that accounts for the non-uniformity of the sediment size
$g_f' = g(\rho_i - \rho_a)/\rho_a$; gravitational acceleration inside the head
H = layer thickness
h_{b0} = initial depth of underflow (can be estimated from the plunge depth)
$h_c = [q_i^2/(g.\varepsilon_i)]^{1/3}$ = critical depth

H_f = actual head height
h_i = inflow depth
$h_n = [q_i^2/(g.\varepsilon_i)]^{1/3}\,[(f_i + f_b)/(8S)]^{1/3}$ = normal depth

h_P = water depth at the plunge point
K = 0.16, parameter coming from laboratory experiments for plane jets for determining the width of an overflow (Safaie 1979)
L_s = overflow length
p_i = fraction of material in the i-th size range present in the bed;
Q_{b0} = revised flow rate including entrainment downstream of the plunge point
q_i = unit width discharge [m^3/s]; (width is the width of the conveyance zone)
Q_i = original inflow rate
$r_{0i} = r_0\, g_0(\delta_i)$, shape factor of the near-bed sediment concentration c_{bi}
r_0 = a shape factor denoting the ratio between the near-bed concentration and the layer averaged concentration for the case of uniform sediment (Parker et al. 1987); laboratory tests have indicated that r_0 is a constant approximately equal to 2. $g_0(\delta_i)$ = a function that accounts for the non-uniformity of the sediment size (Garcia 1994)
R_n = normal depth Richardson number
S = bed slope

S_1, S_2 = profile constant 0.25/0.75 (Ellison and Turner 1959)
T = time
U = layer-averaged velocity in x-direction
u = local velocity in x-direction, averaged over turbulence
u_* = bed shear velocity
u_b = underflow velocity
u_{b0} = mean velocity of the underflow
U_f = velocity of the head
u_i = inflow velocity
u_s = propagation speed of the front ($u_s = q_i/h_s$)
V = mean velocity
v_{si} = fall velocity of sediment in i-th size range
$v_{si}(E_{si}^* - c_{bi})$ = difference between the erosion rate of sediment from the bed and the deposition rate of sediment on the bed, i.e. the net rate of incorporation of bed material of the i-th size range into the flow
W_0 = initial width
W_C = width of the zone of conveyance (the zone where the density current flows)
W_x = width at distance x
x = distance from source
x_0 = reference point for beginning of the underflow
α = f_i/f_b ($0.2 < \alpha < 0.8$)
β = coefficient in entrainment equation (Ashida and Egashira 1977)
γ = (initial) mixing coefficient (is expected to be a function of the densimetric Froude number) $\gamma = 1.2\ F_n - 0.2$; for $F_n > 0.167$ (Jirka and Watanabe 1980)
ε_i = $\Delta\rho_i/\rho_a$ = relative density difference
$\eta^3 C_K$ = mixing efficiency (= 3.2 based on the field studies of Hebbert et al. 1979)
δ_i = D_i/D_{sg} = normalized grain size
ρ_a = density of the ambient water (reservoir)
ρ_i = density of inflowing/turbid water
ρ_s = density of the sediment
$\Delta\rho$ = submerged specific gravity of sediment; $\Delta\rho = (\rho_s - \rho_a)/\rho_a$
$\Delta\rho_i$ = $(\rho_i - \rho_a)$
ρ_{b0} = revised inflow density after entrainment at the plunge point

$$\rho_{b0} = \frac{\gamma \rho_a + \rho_i}{(1+\gamma)}$$

ψ = $Uh\ \Sigma C_i = \Sigma\psi_i$ = volumetric sediment discharge per unit width of the turbidity current
ψ_{ei} = $p_i\ E_{si}\ Uh/r_{0i}$ corresponds to the equilibrium value of the sediment discharge of material in the i-th size range ψ_i (i.e. the value at which erosion and deposition balance) for the local values of flow velocity U and thickness h

10 Literature

Akiyama, J., and Stefan, H.G. (1985). "Turbidity current with erosion and deposition." J. Hydr. Eng. ASCE 111(12), 1473-1496.

Akiyama, J., and Stefan, H.G. (1986). "Prediction of turbidity currents in reservoirs and coastal regions." In: River Sedimentation, vol. III, S.Y. Wang et al. (eds.), Proc. of the 3rd Int. Symp. on River Sedimentation, Univ. of Mississippi, 1295-1305.

Akiyama, J., and Stefan, H.G. (1987). "Onset of underflow in slightly diverging channels" J. Hydr. Eng. ASCE 113(7), 825-844.

Akiyama, J., and Stefan, H.G. (1988). "Turbidity current simulation in a diverging channel." Water Resources Research 24(4), 579-587.

Alavian, V., Jirka, G.H., Denton, R.A., Johnson, M.C., Stefan, H.G. (1992). "Turbidity currents entering lakes and reservoirs". J. Hydraulic Engineering, Vol. 118, No. 11, 1464-1489

Altinakar, S., Graf, W.H., and Hopfinger, E.J. (1990). "Weakly depositing turbidity current on a small slope". J. Hydr. Res. IAHR, 28(1), 55-80.

Bournet, P.E., Dartus, D., Tassin, B., Vincon-Leite, B. (1999). "Numerical investigation of plunging density current". J. Hydraulic Engineering, Vol. 125, No. 6, June, 584-594

Bradford, S.F., Katopodes, N.D., Parker, G. (1997). "Characteristic analysis of turbid underflows". J. Hydraulic Engineering, Vol. 123, No. 5, 420-431.

Chen, Y.H., Lopez, J.L., Richardson, E.V. (1978). "Mathematical modeling of sediment deposition in reservoirs". J of the Hydraulic Division, Dec. 1978, HY 12, S 1605-1616

Chikita, K. (1990). "Sedimentation by river-induced turbidity currents: field measurements and interpretation". Sedimentology, 37, 891-905

Chikita, K. (1989). "A field study on turbidity currents initiated from spring runoffs". Water resources Research, Vol. 25, No. 2, 257-271

Chikita, K. (1992). "The role of sediment-laden underflows in lake sedimentation:glacier-fed Peyto Lake, Canada". J. Fac. Sci., Hokkaido Univ., Ser. VII (Geophysics), Vol. 9, No. 2, 211-224

Chikita, K., Yonemitsu, N., Yoshida, M. (1991). "Dynamic sedimentation processes in a glacier-fed lake, Peyto Lake, Alberta, Canada". Jpn. J. Limnol., 52,1, 27-43

Ellison, T.H., Turner, J.S. (1959). "Turbulent entrainment in stratified flows". Journal of Fluid

Mechanics, Vol. 6, 423-448

Fan, J. (1986). "Turbid density currents in reservoirs". Water International IWRA 11(3), 107-116.

Ford, D.E., Johnsons, M.C. (1983). "Assessment of reservoir density currents and inflow processes". US Army Engineer Waterways Experiment Station, Environmental Laboratory, Technical Report E-83-7

Garcia, M. (1990). "Depositing and erodig sediment-driven flows: turbidity currents". University of Minnesota, St. Anthony Falls Hydraulic Laboratory, Project Report No. 306

Garcia, M., Parker, G. (1991). "Entrainment of bed sediment into suspension". J. Hydraulic Engineering, Vol. 117, No.4, 414-435
Garcia, M., Parker, G. (1993). "Experiments on the entrainment of sediment into suspension by a dense bottom current". J. of Geophysical Research, Vol. 98, No. C3, 4793-4807

Garcia, M., Yu, W., Parker, G. (1986). "Experimental study of turbidity currents". In: Stefan, H.G. et al. (Ed.), Advances in Aerodynamics, Fluid Mechanics and Hydraulics. Proceedings Conf. ASCE, Minneapolis, Minnesota, 120-127

Garcia, M.H. (1993). "Hydraulic jumps in sediment-driven bottom currents". J. Hydraulic Engineering, Vol. 119, No. 10, 1094-1117

Garcia, M.H. (1994). "Depositional turbidity currents laden with poorly sorted sediment". J. Hydraulic Engineering, Vol. 120, No. 11, 1240-1263

Garde, R.J., Ranga Raju, K.G. (1977). "Mechanics of sediment transportation and alluvial stream problems", Wiley Eastern Limited

Graf, W.H. (1983). "The behavior of silt laden currents". Int. Water Power and Dam Construction 35(9), 33-38.

Graf, W.H. (1983). "The hydraulics of reservoir sedimentation". Int. Water Power and Dam Construction 35(4), 45-52.

Hamblin, P.F., Carmack, E.C. "River-induced currents in a Fjord Lake". Journal of Geophysical Research, Vol. 83, No. C2, 1978, 885-899

Hauenstein, W., and Dracos, Th. (1984). "Investigation of plunging density currents generated by inflows in lakes". J. Hydr. Res. IAHR, 22(3), 157-179.

Hay, A.E. (1983). "On the frontal speeds of internal gravity surges on sloping boundaries". Journal

of Geophysical Research, Vol. 88, No. C1, 751-754

Hay, A.E. (1987). "Turbidity currents and submarine channel formation in Rupert inlet, British Columbia". J. Geophys. Res. 92(C3), 2883-2900.

Hebbert, B., Imberger, J., Loh, I., Patterson, J. (1979): "Collie river underflow into the Wellington Reservoir". Journal of Hydraulic Division, ASCE, 105 (HY5), 533-545

Huang, X., Garcia, M. (1997). "A perturbation solution for Bingham-Plastic mudflows". J. Hydraulic engineering, Vol. 123, No. 11, 986-994

Huang, X., Garcia, M. (1998). "A Herschel-Bulkley model for mud flow down a slope". J. Fluid Mechanics, Vol. 374, 305-333

Huang, X., Garcia, M. (1999). "Modeling of non-hydroplaning mudflows on continental slopes". Marine Geology, 154, 131-142

Imberger, J., Patterson, J., Hebbert, B., Loh, I. (1978):"Dynamics of Reservoir of Medium Size". Journal of the Hydraulic Division, ASCE, HY5, 725-743

Lin, C.-P., and Mehta, A.J. (1986). "Sediment-driven density fonts in close canals". Physics of shallow estuaries and bays, J. Van de Kreeke (ed.), Lecture Notes on Coastal nad Estuarine Studies, Springer-Verlag, 159-271.

Luthi, S. (1981). "Experiments on non-channelized turbidity currents and their deposits". Marine Geology 40, Letter Section, M59-M68.

Parker, G., Fukushima, Y., Pantin, H.M. (1986). "Self-accelerating turbidity currents". J. Fluid Mechanis, Vol. 171, 145-181

Parker, G., Garcia, M., Fukushima, Y., Yu, W. (1987). "Experiments on turbidity currents over an erodible bed", J. of Hydraulic Research, Vol. 25, No. 1, 123-147

Sherman, F.S., Imberger, J., Corcos, G.M. (1978) "Turbulence and mixing in stable stratified waters". Annual Review Fluid Mechanics, 1978, 10, 267-288